A HG-IFE-PIC MODEL FOR ION THRUSTER PLUME INTERACTIONS

J. Wang and R. Kafafy

Virginia Polytechnic Institute and State University, Blacksburg, VA 24061, USA

Abstract

This paper presents a new algorithm, the hybrid-grid immersed-finite-element particle-in-cell, for modeling electric propulsion plume spacecraft interactions. This algorithm is designed to handle the complex boundary condition of a real spacecraft accurately while maintaining the computational speed of a standard PIC code. Simulations are performed to study multiple-ion thruster plume spacecraft interactions.

1. Introduction

Electric propulsion is now considered a critical enabling technology for many future space missions. An electric propulsion device propels a spacecraft by continuously emitting a high speed plasma flow over long periods of time. Effects from electric propulsion plume have long raised both engineering and science concerns. Engineering concerns include plume contamination on spacecraft surfaces and sensors and spacecraft interactions with the induced plasma environment. Science concerns include plume effects on measurements of ambient plasma and magnetic fields to be measured. A long standing question in electric propulsion is how does one quantitatively predict the effects from thruster plume on spacecraft and science measurement to ensure that spacecraft reliability and science return would not be compromised?

There have been significant efforts in research related to electric propulsion plume effects. Although ground based experimental plume studies started in the 1960's (for example, see [Carruth, 1981] and references therein), investigating plume-spacecraft interactions in a vacuum tank remains to be a challenging endeavor to this day due to the intrinsic complex nature of spacecraft-plume interactions, the difficulty of matching in-space conditions in a laboratory, and effects from test chamber and diagnostic techniques. On the other hand, the cost associated with performing space experiments and a lack of flight opportunity precludes using in-flight investigation to study most interaction scenarios. It has been recognized that first-principle based models using computer particle simulations provides one of the best means to quantify the effects of electric propulsion.

Numerous electric propulsion plume models have been developed in recent years. As an example, Wang et al[2001] developed a 3-dimensional particle simulation model for ion thruster plume which is in excellent agreement with in-flight plume measurements from the Deep Space 1 spacecraft. These models involves few assumptions, focus on the detailed physics but are much more computational intensive. Due to computational limitations, most existing particle simulation based plume models involve simplified spacecraft configurations and particle simulations are often performed using relatively small simulation domains. Hence, existing models are mostly used as research tools rather than engineering tools. In order to develop an engineering design tool using particle simulations, one needs to be able to build up a code that is sophisticated enough so the complex geometry associated with a spacecraft and all the physics can be modeled properly and yet computationally efficient enough so large-scale 3-D particle simulations can be performed routinely. However, accuracy and computing speed often represent conflicting requirements for a PIC code. In the presence of a complex geometric boundary, the electric field can be solved very accurately using an unstructured mesh to body fit the object. However, this approach can be very expansive for particle push. Particle push is most efficient when using a Cartesian mesh, but a standard finite-difference Cartesian mesh based field solver will lose accuracy in the vicinity of the boundary.

This paper presents a new PIC algorithm, the hybrid-grid immersed-finite-element particle-in-cell (HG-IFE-PIC), for modeling electric propulsion plume interactions. This algorithm is designed to handle the complex boundary condition of a real spacecraft accurately while maintaining the computational speed of a standard PIC code. Section 2 discusses this algorithm. Section 3 applies the new model on simulations of multiple-ion thruster plumes. Section 4 contains a summary and conclusions.

2. Algorithm

2.1. Immersed-Finite-Element Formulation

The simulation model is based on the immersed finite element (IFE) formulation. The IFE formulation offers many advantages for use in a PIC code. The primary attraction is that mesh can be independent of the object boundary. Specifically, it allows one to use a fixed Cartesian mesh to solve problems involving complex geometric boundary or even time-varying boundary with the same accuracy as a body fit mesh with second order converge rate [Kafafy et al., 2005]. Additionally, the electric field can be solved for both inside and outside of the object if needed and thus the effects from the material properties at surface on electric field can be explicitly included. This method also has several nice mathematical properties. For instance, the involved algebraic systems in the IFE method are symmetric and positive definite. When a structured mesh is used, the algebraic systems involved will also have the usual nice sparse banded structure. This allows easy implementation of fast solution techniques such as preconditioned conjugate gradient and multi-grid methods, and domain decomposition techniques for parallel computers.

The IFE-PIC model uses a structured Cartesian-tetrahedral mesh. The Cartesian mesh is the primary mesh used by PIC. Each Cartesian cell is further divided into five tetrahedral elements as shown in Fig. 1. The tetrahedral mesh is the secondary mesh used only by the IFE field solver. When a curved object surface is present, the IFE mesh will include both interface cells (those cells that have at least one edge whose interior intersects with the interface) and non-interface cells. In a non-interface cell, the standard linear local nodal basis functions can be used to span the local finite element space. In an interface cell, the physical jump conditions at interface are used to determine the basis function. The details of the IFE based field solver can be found in [Kafafy et al., 2005].

2.2. Hybrid-Grid IFE-PIC

The plume-spacecraft interaction problem involves not only complex boundary condition but also a non-uniform plasma. In order to solve the expansion of the charge-exchange plasma more efficiently, we further make the IFE mesh and the PIC mesh completely independent from each other. We maintain a Cartesian mesh for PIC but stretch the primary Cartesian cell in the IFE field solver according to the local potential gradient and plasma density. This algorithm is referred to as the hybrid-grid IFE-PIC (HG-IFE-PIC). The application of the hybrid grid reduces the elements used by the IFE field solver in the far-field region and thus can significantly reduce the computational time.

The IFE mesh is stretched in each coordinate independently according to the following stretching rule

$$\frac{x(\zeta)-x_0}{L}=\frac{\beta+1-(\beta-1)\left(\frac{\beta+1}{\beta-1}\right)^{1-\zeta}}{\left(\frac{\beta+1}{\beta-1}\right)^{1-\zeta}+1}$$

where x is the physical coordinate, ζ is a logical coordinate such that $0 \le \zeta \le 1$, and β is a stretching parameter such that $\beta > 1$. Note that $x(0)=x_0$, $x(1)=L$.

The HG-IFE-PIC requires two mesh-mesh interpolation steps to transfer information between the PIC mesh and the IFE mesh in addition to the particle-mesh interpolations used by a PIC code. In a simulation, the charges of simulation particles are first deposited onto the PIC mesh using the typical linear weighting functions of a standard PIC code. These quantities are then interpolated from the PIC mesh onto the IFE mesh through linear interpolation before field solve (Note that the IFE mesh size should be no smaller than the PIC mesh size.). The electric field are obtained on the IFE mesh during the field solve. After the field solve, the electric field quantities are interpolated from the IFE mesh onto the PIC mesh for particle push. The IFE to PIC mesh interpolation uses the finite element basis functions constructed on the IFE mesh

$$u_{i,j} \sum_{k=1}^{4} u_k \psi_k(\bar{x}_{i,j})$$

where $u_{i,j}$ is the field quantity u interpolated at the PIC mesh node (i,j), u_k is the field quantity evaluated at the IFE mesh element node k and $\psi_k(x_{i,j})$ is the IFE local basis function k evaluated at the PIC mesh node location $x_{i,j}$. The three interpolation procedures are illustrated in Figure 2.

3. Modeling Multiple Ion Thruster Plume Interactions

3.1 Simulation Model

The HG-IFE-PIC algorithm is applied to develop a three-dimensional electrostatic PIC model for ion thruster plume-spacecraft interactions. The simulation is run in two phases. The first phase simulates the charge-exchange plasma. The physical model for charge-exchange plasma simulation is the same as that described in [Wang et al., 2001]. In this code, only the charge-exchange ions are treated as test particles. The electrons are assumed to be an isothermal fluid and the beam ion density is modeled analytically. The code solves self-consistently the particle trajectories and space charge for the charge-exchange plasma and the electric field surrounding the spacecraft. The second phase simulates plume contamination on spacecraft using the steady state solution of the charge-exchange plasma simulation. The contamination run traces the trajectories of the ionized sputtered particles.

In this paper, we consider three spacecraft models, as shown in Figure 3. The spacecraft bus is taken to have a configuration similar to the DAWN spacecraft, a cube with a side length of about 1.3m plus a spherical antenna dish, a solar array, and some payloads. In the three models considered here, we assume the spacecraft bus is attached to one ion thruster (model 1), three ion thrusters (model 2), or four ion thrusters (model 3), respectively. The thrusters are assumed to be the 30cm diameter NSTAR ion thruster.

Similar to [Wang et al., 2001], the input parameters for charge-exchange simulation include the ion beam density and neutral plume density at thruster exit (derived from DS1 ion engine operating condition for ML 83), the potential difference between the plume and spacecraft ground and the electron temperature in the plume (assumed to have the values measured by DS1 IDS instrument), and charge-exchange collision cross section. The spacecraft surface is assumed to have a uniform potential distribution equal to the spacecraft ground. For the contamination simulation, we utilize the acceleration grid current measured during NSTAR thruster ground test, measured ion sputtering yield, and the Xe-Mo charge-exchange collision cross section measured in [Rutherford and Vroom, 1981] to calculate the Mo ion production rate.

The simulation mesh is shown in Figure 4. The PIC mesh is a uniform Cartesian mesh of $105 \times 54 \times 90$ cells. Each cell is a 6-cm cube. The cell size is selected to resolve the Debye length of the CEX plasma in the wake region. The IFE field solver uses a two-zone mesh. The inner-zone surrounds the spacecraft bus, has no stretching and has a Cartesian cell size equal to the PIC cell size. The outer zone is stretched according to the stretching rule in Section 2 in all directions. The entire IFE mesh has 830,465 tetrahedral elements. A simulation typically uses 5–6 million particles. The charge-exchange plasma simulation typically takes less than 4 hours on a Pentium 4 PC at 2.2 GHz, while the contamination run takes less than an hour.

3.2 Simulation Results

Results for three simulation cases are shown in Figures 5 through 10. Simulation case 1 concerns spacecraft model 1 with single thruster firing, case 2 concerns spacecraft model 2 with three thrusters firing simultaneously, and case 3 concerns spacecraft model 3 with four thrusters firing simultaneously. Results from charge-exchange plasma simulation show the expansion characteristics obtained in [Wang et al., 2001]. However, the presence of the antenna dish enhances the backflow, as the antenna is assumed to have the spacecraft ground potential.

A primary concern for space missions using ion propulsion is contamination caused by the sputtered grid material, Mo. The sputtered Mo atoms can become ionized due to charge-exchange collisions with the propellant ions or electron impact collision and backflow to contaminate spacecraft surface. In particular, deposition of contaminants on solar cell can cause power loss, temperature change, or even catastrophic shorting of the circuit. Figures 6, 8 and 10 show the trajectories of Mo ions and the deposition rate of Mo ions on spacecraft surface measured in A° per thousand hour of thruster operation. The simulations show that the average deposition of Mo ions on solar array surface is on the order of 10^{-2} A° per thousand hour of thruster operation, posing a moderate contamination risk. It is also interesting to note that contamination from a cluster of thruster is not a simple of sum of the contaminations from single thrusters. The major factor that influences the backflow for both the charge-exchange Xe ions and the ionized Mo particles is the relative position of thruster with respect to the spacecraft.

4. Summary and Conclusions

In summary, a 3-D HG-IFE-PIC algorithm is developed to hand problems involving complex boundary conditions and non-uniform plasmas. We find the IFE field solver has the same accuracy as a body-fit mesh based solver with second order of convergence and the computational speed of the HG-IFE-PIC code is close to a standard PIC code. The IFE formulation allows an easy deployment of fast solution techniques for the Poisson's equation and easy implementation on parallel computers. The HG-IFE-PIC algorithm is applied to develop a simulation model for ion thruster plume spacecraft interactions. Simulations are performed for spacecraft with multiple ion thrusters. We find that the contamination effects from NSTAR thruster on the solar array is very moderate. For a multiple thruster configuration, the contamination deposition on solar array in general is not the sum of the contamination produced by individual thrusters. The dominating factor influencing contamination is the relative position of thruster with respect to spacecraft

5. References

Carruth, M.R., Editor, Experimental and Analytical Evaluation of Ion Thruster/Spacecraft Interactions, *JPL Publication* 80-92, 1981.

R. Kafafy R., T. Lin, Y. Lin, and J. Wang, "3-D Immersed Finite Element Method for Electric Field Simulation in Composite Materials", *Int. J. Numerical Methods in Engineering* (accepted), 2005.

J.A. Rutherford and D.A. Vroom, *J. Chem. Phys.*, 74(1), 1981, pp434.

Wang, J., D. Brinza, and M. Young, "Three-Dimensional Particle Simulation Modeling of Ion Propulsion Plasma Environment for Deep Space 1", *J. Spacecraft & Rockets*, 38(3), 2001, pp433--440.

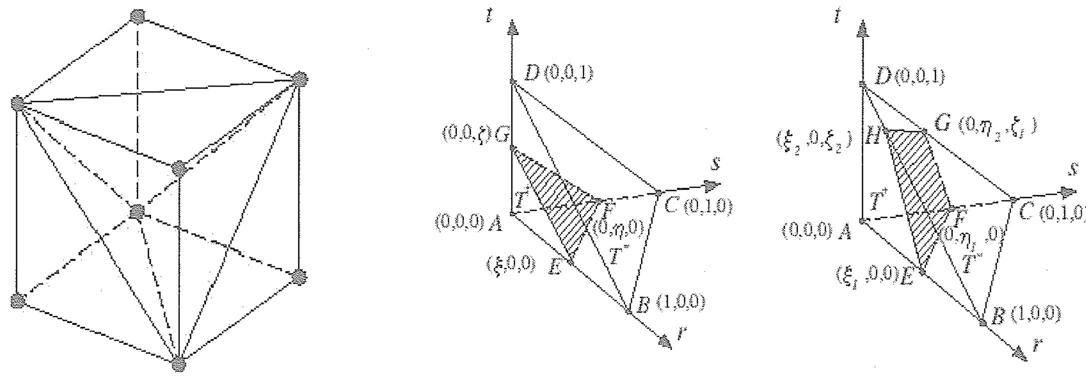

Fig. 1: The Cartesian-tetrahedral cell used by IFE-PIC and intersection topologies of a tetrahedral element

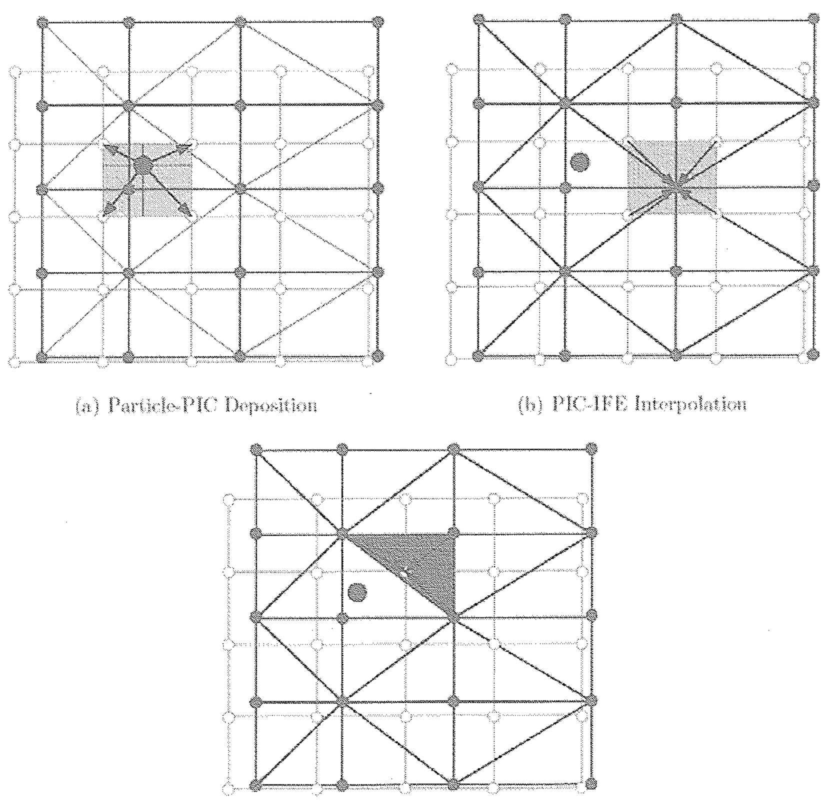

(a) Particle-PIC Deposition

(b) PIC-IFE Interpolation

(c) IFE-PIC Interpolation

Fig. 2: Interpolation procedure of the HG-IFE-PIC code

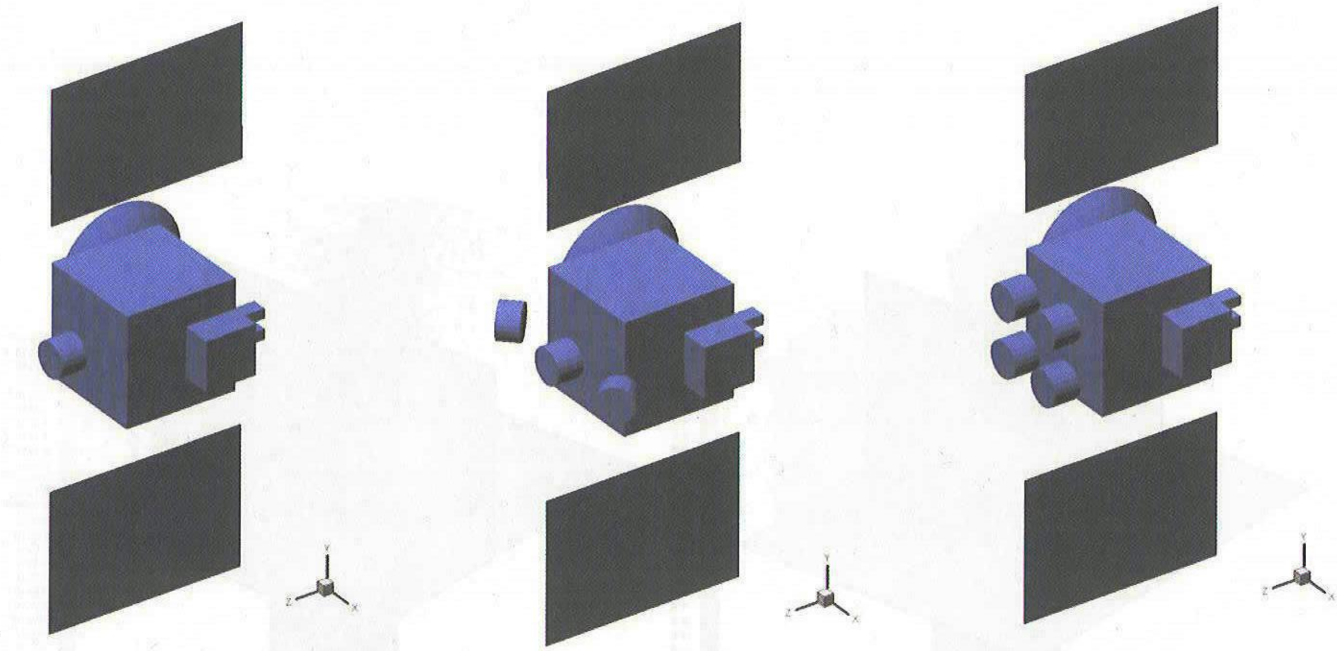

Model 1 **Model 2** **Model 3**

Fig. 3: Spacecraft model

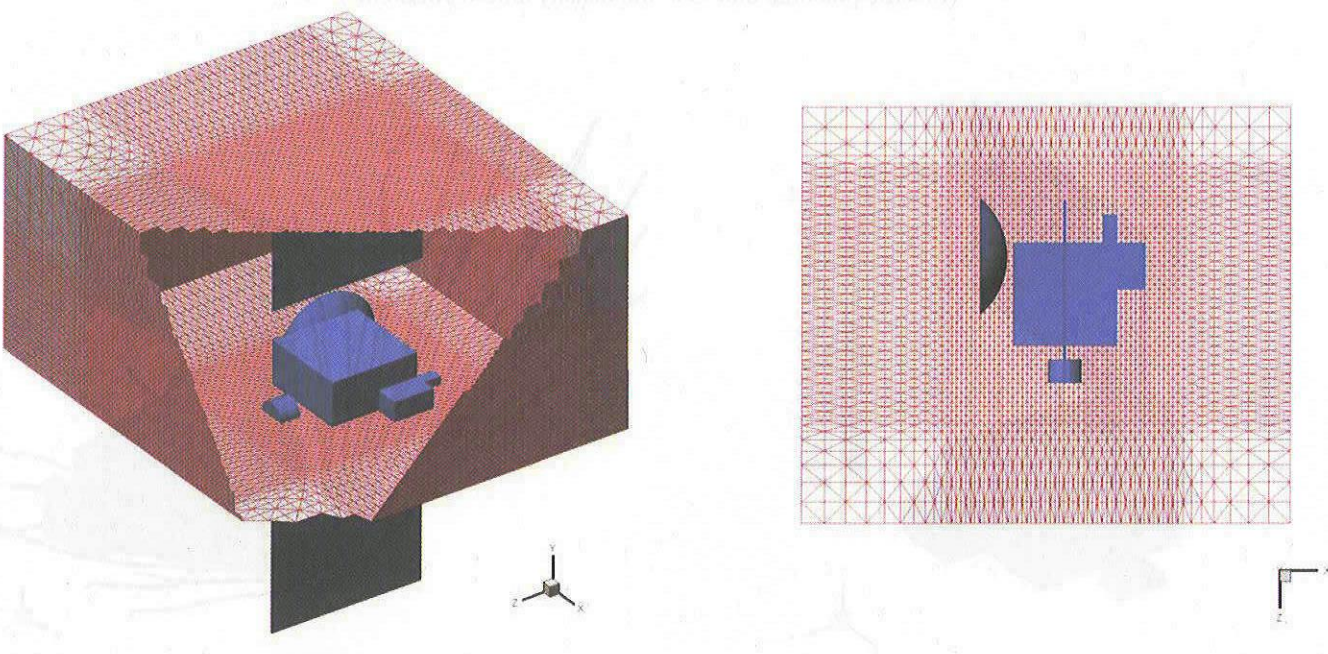

Fig. 4: Simulation mesh

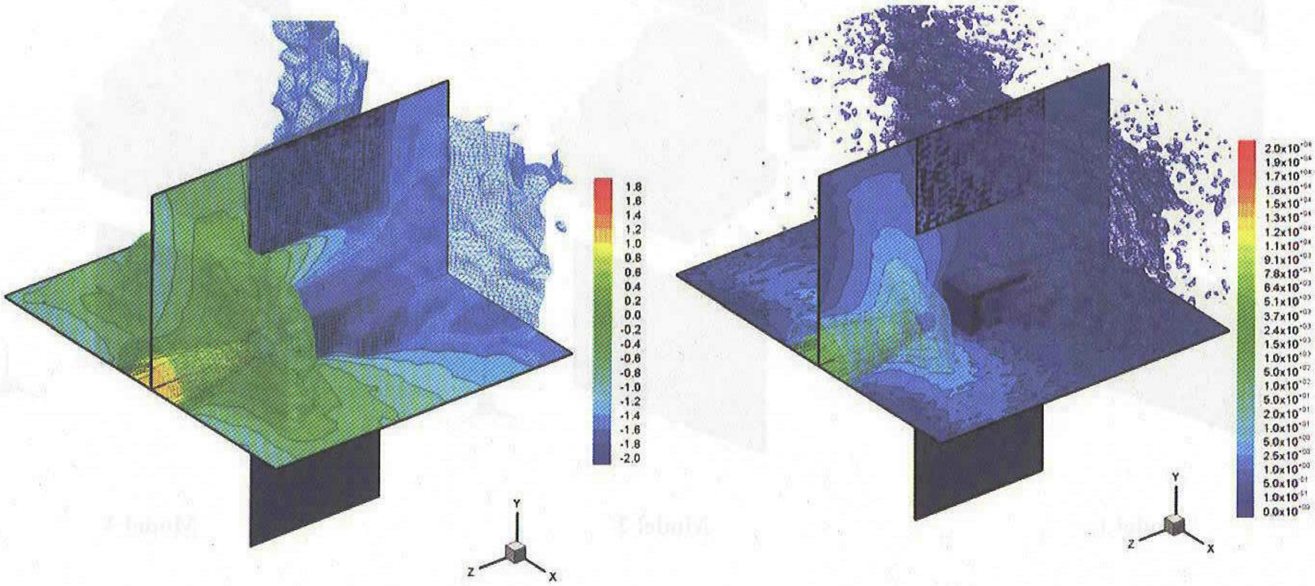

Fig. 5: Case 1 charge-exchange plasma simulation. Normalized electric potential (left) and ion density contours (right) (Electric potential unit=5V. Ion density unit=0.76E5/cm^3)

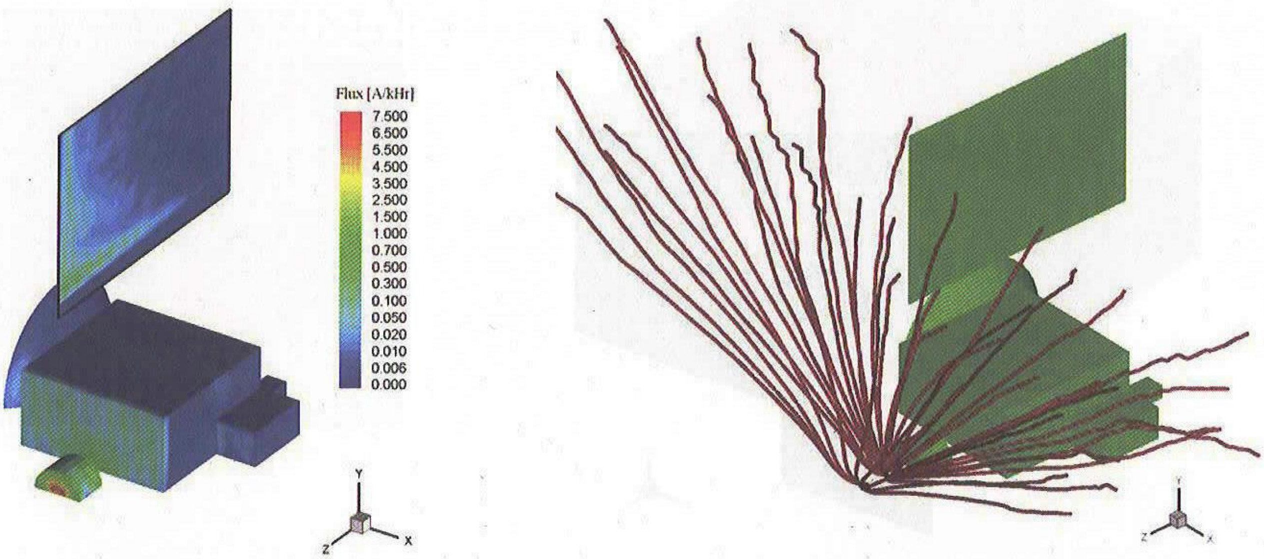

Fig. 6: Case 1 contamination simulation. Contamination deposition (left) and contaminate trajectories (right)

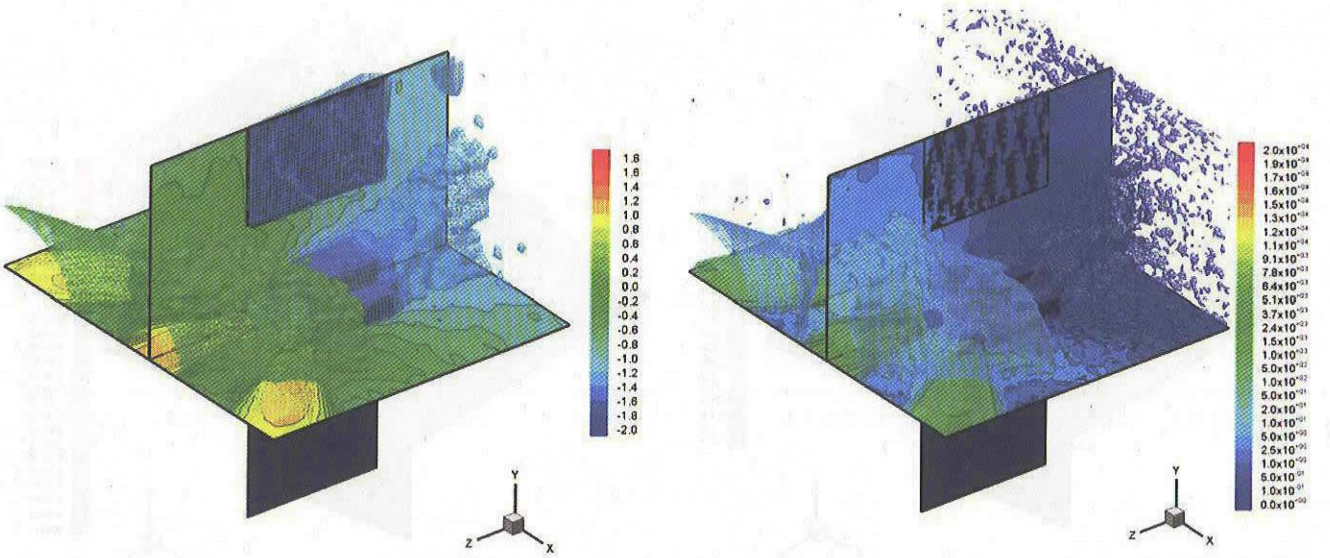

Fig. 7: Case 2 charge-exchange plasma simulation. Normalized electric potential (left) and ion density contours (right) (Electric potential unit=5V. Ion density unit=0.76E5/cm^3)

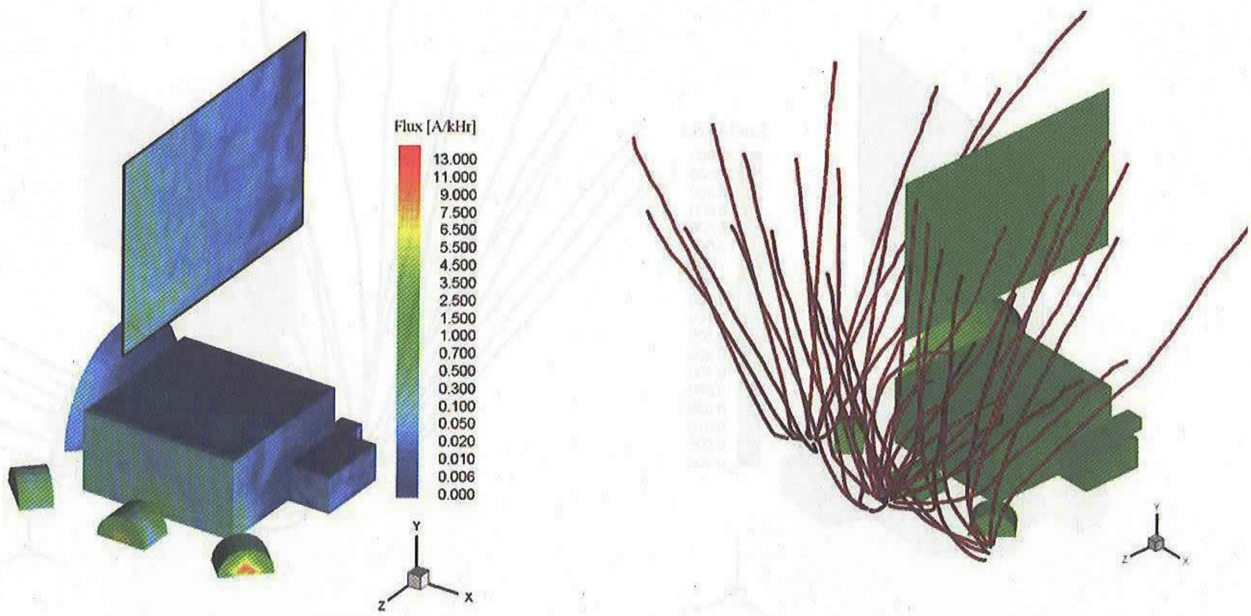

Fig. 8: Case 2 contamination simulation. Contamination deposition (left) and contaminate trajectories (right)

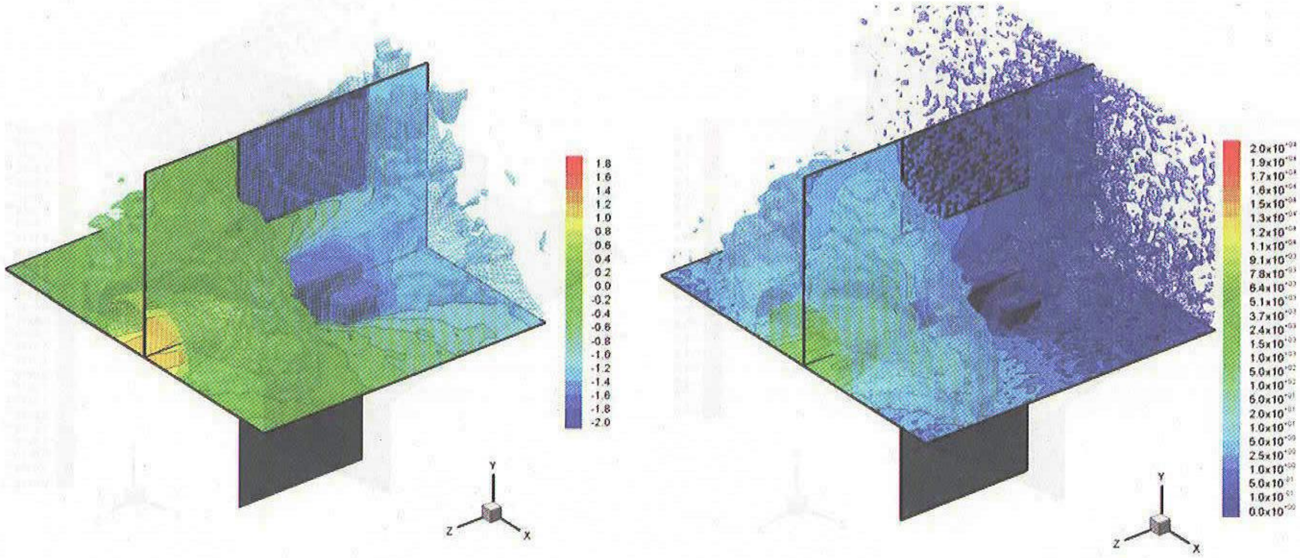

Fig. 9: Case 3 charge-exchange plasma simulation. Normalized electric potential (left) and ion density contours (right) (Electric potential unit=5V. Ion density unit=0.76E5/cm^3)

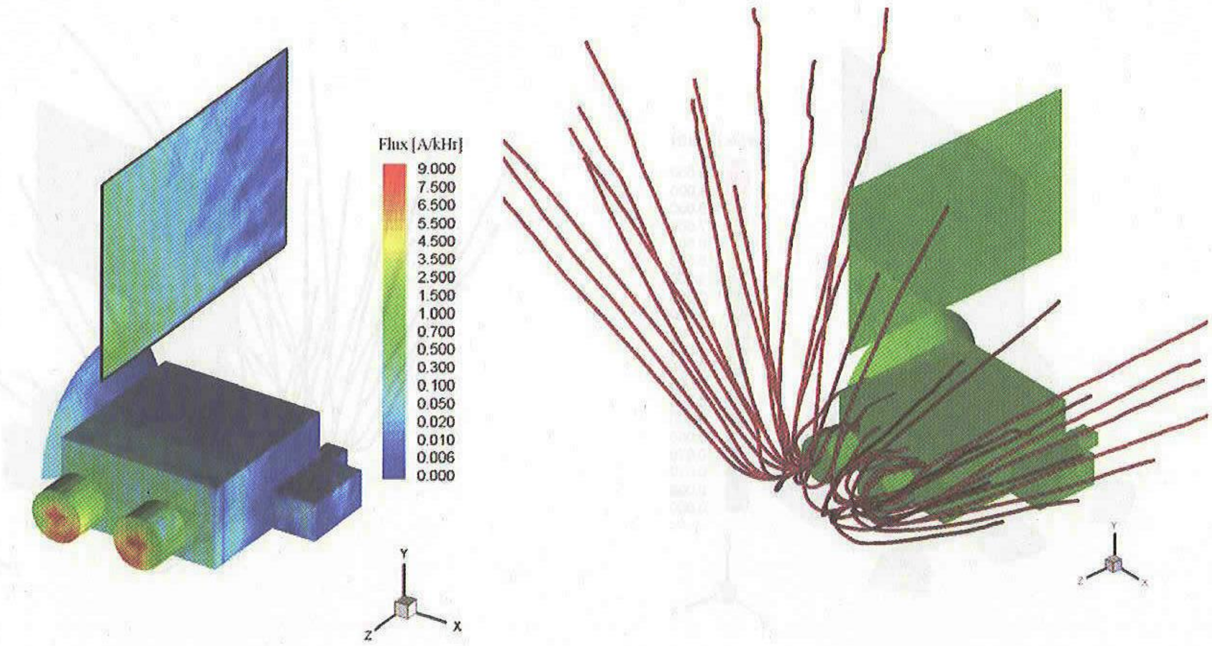

Fig. 10: Case 3 contamination simulation. Contamination deposition (left) and contaminate trajectories (right)